Proceedings of ICRC 2001: 4015 © Copernicus Gesellschaft 2001

ICRC 2001

Simulation of the solar proton dose observed during the STS-28 flight

D. F. Smart[1], M. A. Shea[1], M. J. Golightly[2], M. Weyland[3], and A. S. Johnson[3]

[1]CSPAR, University of Alabama, Huntsville, AL 35899, USA
[2]NASA Johnson Space Center, SN31, Houston, TX 77058, USA
[3]Lockheed Martin, NASA Johnson Space Center, Houston, TX 77058, USA

Abstract. We present comparisons of the radiation dose measured on the space shuttle during the 12-13 August 1989 solar proton event with the dose computed from solar particles predicted to be allowed through the magnetosphere to the space shuttle position. We have developed a dynamic cutoff rigidity model indexed by integer values of the Kp magnetic index to specify the vertical cutoff rigidities derived from employing the Tsyganenko magnetospheric model. We find a one-to-one correspondence between the portion of the orbit predicted to be subjected to solar protons and the portion of the orbit where solar particle dose measurements were obtained.

1 Introduction

We have a complete set of world grids of vertical cutoff rigidities each 5° in latitude and 5° in longitude for a spacecraft orbiting at 450 km. This reference set of world grids covers all magnetic activity levels from super quiet to extremely disturbed (i.e., Kp indices ranging from 0 to 9^+). These world grids of vertical cutoff rigidities were obtained by particle trajectory tracing in model magnetospheres.

1.1 Magnetospheric Models

We used the Tsyganenko (1989) magnetospheric field model combined with the International Geomagnetic Reference Field for Epoch 1995.0 (Sabaka et al., 1997) in the manner described by Flückiger and Kobel (1990). The magnetic fields utilized were defined for 1 January 1995. The Tsyganenko (1989) magnetospheric field model describes the magnetospheric field topologies for Kp magnetic indices from 0 to 5.

Correspond to: sssrc@msn.com

The Boberg et al. (1995) extension was used to describe the magnetospheric fields for magnetic activity levels exceeding Kp values of 5. For convenience we have labeled these as Kp 6 through 10 for Dst increments of -100 nT.

1.2 Cutoff Rigidity Determination Procedure

Cosmic ray trajectory calculations were initiated in the vertical direction from a distance of 6821.2 km from the geocentric (450 km altitude above the average earth radius of 6371.2 km). The "sensible" atmosphere of the earth was considered to extend 20 km above the international reference ellipsoid, and any trajectory path that came lower than this distance was considered to be re-entrant and hence forbidden. In this work "vertical" is the direction radial from the earth center. We utilized the Bulirsch-Stoer numerical integration technique (Press et al., 1989) to minimize the number of steps required in a charged particle trajectory computation. Each step length was about 1% of a gyro-distance (Smart and Shea, 1981), the distance the particle of the specified rigidity would travel during one gyration in a uniform magnetic field of the same intensity.

The cutoff rigidities are determined by calculating charged particle trajectories at discrete rigidity intervals starting with a rigidity value high above the highest possible cutoff and decreasing the rigidity to a value that satisfied our criteria that the lowest allowed trajectory had been calculated. As the calculations progress down through the rigidity spectrum, the results change from the easily allowed orbits to a complex structure of allowed, forbidden, and quasi-trapped orbits (loosely called penumbra) and finally to a set of rigidities where all trajectories intersect the solid earth. Rigidity interval spacing of 0.01 GV was used throughout the cosmic ray penumbra. As a result of these trajectory calculations we determined the calculated upper cutoff rigidity (R_U) which is the rigidity value of the highest allowed/forbidden pair of adjacent cosmic ray trajectories, the calculated lowest cutoff rigidity (R_L) which is the rigidity value of the lowest allowed/forbidden pair of adjacent cosmic ray trajectories, and an "effective cutoff rigidity" (R_C) found by summing the allowed orbits through the penumbra as described by Shea et al. (1965).

See Cooke et al. (1991), for definitions of cosmic ray cutoffs.

2 The Dynamic Cutoff Rigidity Model

These updated cutoff rigidity models have a 5 degree by 5 degree world grid spacing which results in better fits to the available data than the course 5 degree in latitude by 15 degree in longitude world girds (Smart et al., 1999a,b,c). A comparison of the components of this dynamic cutoff rigidity model with vertical cutoff rigidities calculated using only an internal geomagnetic field for the same altitude (Smart and Shea, 1997) show that these magnetospheric cutoff rigidity values are consistently lower in magnitude, even for the Kp=0 case.

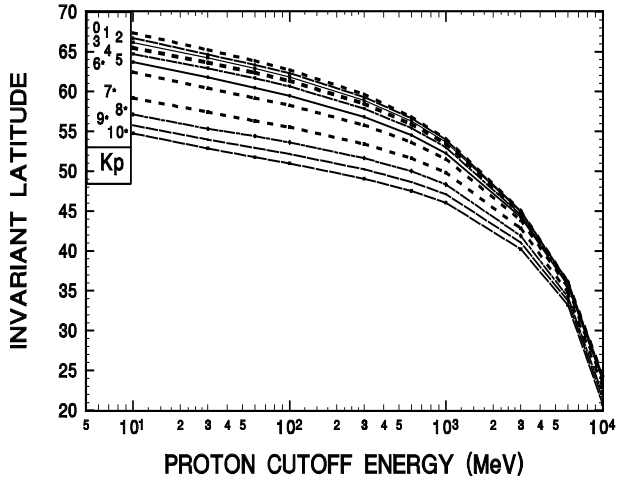

Fig. 1. Change in effective vertical cutoff energy at 450 km altitude as a function of magnetic activity.

Rigidity is not the most convenient unit for use with energetic particle data since most energetic particle measurements are in units of energy. For comparison purposes, we have selected the invariant latitude calculated from the internal geomagnetic field as a common parameter. We have interpolated through our world grids of vertical geomagnetic cutoff rigidities for each magnetic activity level to determine proton cutoff energy contours as a function of invariant latitude and obtained an average invariant latitude for each energy. The proton cutoff invariant latitudes as a function of magnetic activity are illustrated in Figure 1. The energy contours in this figure are the average of cutoff calculations at four different universal times, 00 UT, 06 UT, 12 UT and 18 UT. These curves indicate an almost linear relation between the proton cutoff energy with latitude in the range from about 10 MeV to a few hundred MeV. We note that the change of proton cutoff energy with Kp is relatively uniform over the range of the original Tsyganenko (1989) model, but the cutoff changes introduced by the Boberg et al. (1995) extension is non-linear with the Dst increment.

3 Comparisons Of Computed Solar Particle Dose With Spacecraft Dosimetry Data

The STS28 space shuttle flight in August 1989 was in a 57º inclination orbit and carried a dosimeter that provided data every 10 seconds of the mission. This flight encountered the beginning of the large solar proton event sequence that began on 12 August 1989 at 15 hours UT and recorded dosimetry data due to solar particles whenever the orbit passed into the low cutoff region at high magnetic latitudes. The STS28 flight was completed on 13 August with the shuttle landing shortly after 13 UT. We will use this dosimetry data acquired during an actual space flight as a method of evaluating the accuracy of the dynamic cutoff rigidity model. During the time the vehicle encountered solar protons, the geomagnetic activity level as quantified by the Kp index varied between 1 and 3 as shown in Table 1.

Table 1. Kp index values for each 3-hour interval, 12 – 13 August 1989.

Date								
12	00	03	06	09	12	15	18	21
	3^-	2	2^-	1^+	2	0^+	1	2
13	00	03	06	09	12	15	18	21
	3^-	2^+	2	2^-	2^+	1	2^-	2^-

The comparison method will apply this dynamic cutoff rigidity model to predict the solar proton transmission through the magnetosphere to the position of the space shuttle (latitude, longitude and altitude) each minute of the shuttle fight during its encounter with the solar proton event. The solar particle flux predicted to arrive to the skin of the space shuttle at each position was transmitted through a model of the physical mass of the shuttle structure to the dosimeter location to generate a computed radiation dose rate for comparison with the actual measured dose rate. A more detailed description of this radiation dose rate calculation method is given by Golightly and Weyland (1997). The general procedure was:

1. Determine (by interpolation in the appropriate 5° x 5° world grid of cutoff rigidities) the vertical cutoff proton energy at the spacecraft position for each minute of the solar proton event encounter.
2. Model the GOES measured solar proton flux as the differential flux impacting the magnetosphere as an exponential fit to the solar particle flux.
3. Determine the differential solar particle flux at energies exceeding the proton cutoff energy at the spacecraft position.
4. Reduce the free space omni-directional flux to account for "earth shadowing" in low-earth orbit.

5. Attenuate the incident solar particles through the spacecraft mass distribution.
6. Calculate the dose rate from the attenuated solar proton flux spectrum penetrating to the dosimeter location.

If the cutoff rigidity has the proper value, then the computed dose rate and the measured dose rate should be very similar.

3.1 Comparisons Using Cutoff Parameters

The STS28 dose rate data set also provided an opportunity to check the applicability of the various cutoff rigidity parameters such as R_U, R_L, and R_C. Use of the vertical upper cutoff rigidity, R_U, (i.e. none of the solar particle flux in the penumbra was used in the dose calculations) resulted in an underprediction of the dose rate at all geomagnetic cutoffs. Use of the lower cutoff rigidity, R_L, (i.e. the penumbra was assumed to be totally transparent and all of the solar particle flux down to R_L was used in the dose calculations) resulted in an overprediction of the dose rate at all geomagnetic cutoffs. Use of the effective cutoff rigidity, R_C, (which uses a linear average the allowed/forbidden regions of the penumbra) resulted in a slight systematic underprediction of the dose rate.

Using all of the solar particle flux down to R_U and 50% of the solar proton flux between R_U and R_L also resulted in a slight systematic underprediction of the dose rate. We found that using all of the solar particle flux down to R_U and then using the average transparency of the penumbra to specify the solar particle flux transmitted through the penumbra between R_U and R_L resulted in a systematically better correspondence between the computed and measured dose rate. This average transparency, a function of the cutoff rigidity, is shown in Figure 2.

3.2 Detailed Comparisons

We specifically examined each high latitude pass (region of lower cutoff rigidity) in order to ascertain the utility of the dynamic cutoff rigidity model. Employing this dynamic cutoff rigidity model with a proper selection of the magnetic activity index (see below) resulted in a one-to-one correspondence between the time periods of computed radiation dose rate due to solar protons being allowed through the magnetosphere to the position of the space shuttle and the measured dose rate in the vehicle, even for very small doses.

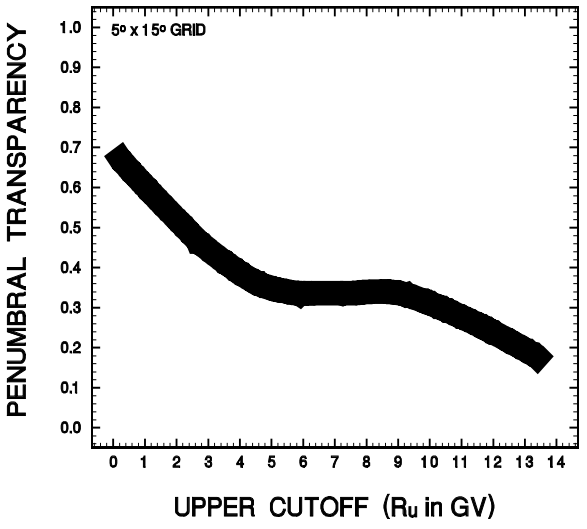

Fig 2. The average transparency of the penumbra as a function of vertical cutoff rigidity

In the analysis done by Golightly and Weyland (1997) using the cutoff rigidities determined from the internal geomagnetic field only, they noted that there were two high latitude passes where there were measurements of solar particle radiation at the spacecraft when the internal geomagnetic field cutoff did not predict a significant solar particle flux to be allowed to the spacecraft position. These occurred at 13 August at 08:13-08:20, and 11:13-11:26. These time periods provide an opportunity to evaluate the selection of the proper index for the dynamic cutoff rigidity model. We have found that truncating the Kp magnetic activity index results in selecting a cutoff value at the spacecraft position that is too high so the solar particle flux predicted to be allowed at the spacecraft is not sufficient to reproduce the dose measurement. We found that it is necessary to "round up" the Kp index in order to compute a cutoff value such that the predicted dose rate is consistent with the measured dose rate.

A detailed examination of the computed dose rate and the observed dose rate at very low cutoff values shows an "overshoot" in the computed dose rate at very low cutoff values. Our investigation into the cause of this overshoot indicates that it is not a result of the geomagnetic cutoff because at the time and position of the overshoot the geomagnetic cutoff values are very low, below the cutoff energy of the mass shielding. Our initial conclusion is that it is the result of using the simple exponential fit between the 30 MeV and 100 MeV solar particle flux to characterize the entire solar particle spectrum. This simple exponential simulation of the solar proton spectrum apparently generates an excess of high-energy protons that are probably not present in the actual solar particle spectrum. We suggest that the streaming limit (Reames and Ng, 1998), a phenomena where at high flux levels the proton self-generated waves affect the particle acceleration and results in a flattening of the lower energy portion of the solar particle spectrum (Reames, 1999), biases the 30 to 100 MeV por-

tion of the spectrum so that this exponential rigidity fit is not truly representative of the entire range of the solar proton flux at higher energies. We found that a multi-section fit of the solar proton energy spectrum (an exponential between 30 and 50 MeV, an exponential fit between 50 and 60 MeV combined with a final exponential fit between 60 and 100 MeV which was then used to extrapolate to higher energies) resulted in a reduction of the overshoot.

Employing the flux spectral correction and the actual Kp magnetic activity given in Table 1 we have computed the solar particle dose rate for each minute of the STS28 flight. The comparison between the computed and measured dose rate is given in Figure 3. Note that a better specification of the particle flux removed the overshoot at very low cutoff values. Also note that underprediction of the dose rate in the interval at12:00-12:10 UT. This is the result of truncating the Kp value (see Table 1). We have found that for this time interval, using the "rounded up" Kp value of 3 instead of the truncated Kp value of 2 results in a better agreement between computed and observed dose rate.

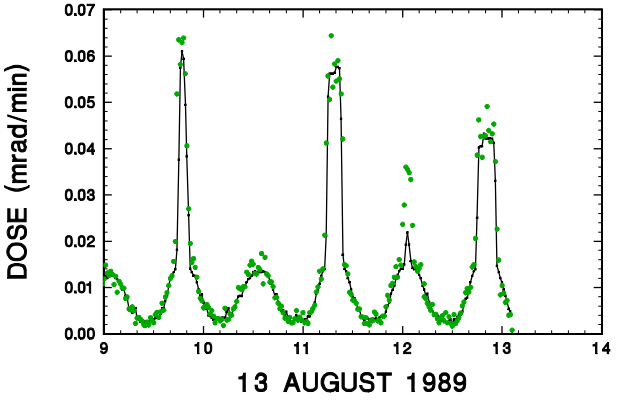

Fig 3. Comparison of computed (solid line) and observed (dots) radiation dose rate during the STS28 encounter with the 13 August 1989 solar proton event.

4 Conclusion

A comparison of the computed and measured radiation dose rate on the STS28 space shuttle encounter with the 12-13 August 1989 solar proton event shows that use of the dynamic cutoff rigidity model where the cutoff rigidity is selected by the magnetic activity index "rounded up" correctly predicts when solar particles were allowed through the magnetosphere to the spacecraft position. The use of this dynamic cutoff rigidity model results in a one-to-one correspondence between the portion of the orbit predicted to be subjected to solar protons and the portion of the orbit where the radiation dose attributed to solar particles was obtained.

Acknowlegement. The trajectory calculations were made at the Maui High Performance Computer Center.

References

Boberg, P.R., A. Tylka, J. Adams, E.O. Flückiger, and E. Kobel., Geomagnetic transmission of solar energetic particles during the geomagnetic disturbance of October 1989, *Geophys. Res. Lett.*, **22**, 1133-1136, 1995.

Cooke, D.J., J.E. Humble, M.A. Shea, D.F. Smart, N. Lund, I.L. Rasmussen, B. Byrnak, P. Goret, and N. Petrou, On cosmic-ray cutoff terminology, *Il Nuovo Cimento C*, **14**, 213-234, 1991.

Flückiger, E.O., and E. Kobel, Aspects of combining models of the earth's internal and external magnetic fields, *J. Geomag. Geoelectr.*, **42**, 1123-1136, 1990.

Golightly, M.J., and M. Weyland, Modeling Exposures Aboard the Space Shuttle from the August 1989 Solar Particle Event, Paper No .13 in *Impact of Solar Energetic Particle Events on Design of Human Missions*, Center for Advanced Space Studies, Houston TX, 1997.

Press, W.H., B.P. Flannery, S.A.Teukolsky, and W.T. Vettering, Numerical Recipes, Cambridge Univ. Press, Cambridge, 1989.

Reames, D.V. and C.K. Ng, Streaming-limited intensities of solar energetic particles, *Astrophy. J.*, **504**, 1002-1005, 1998.

Reames, D.V., Particle acceleration at the sun and in the heliosphere, *Space Sci. Rev*, **90**, 413- 491, 1999.

Sabaka, T.J., R.A. Langel, R.T. Baldwin, and J.A Conrad, The geomagnetic field, 1900-1995, including the large scale fields from magnetospheric sources and NASA candidate models for the 1995 IGRF revision, *J. Geomag. Geoelect.*, **49**, 157-206, 1997.

Shea, M.A., D.F. Smart, and K.G. McCracken, A study of vertical cutoff rigidities using sixth degree simulation of the geomagnetic field, *J. Geophys. Res.*, **70**, 4117-4130, 1965.

Smart, D.F. and M.A. Shea, Optimum step length control for cosmic ray trajectory calculations, *Proc. 17th ICRC*, **4**, 255-258, 1981.

Smart, D.F. and M.A. Shea, Calculated cosmic ray cutoff rigidities at 450 km for epoch 1990, *Proc. 25th ICRC*, **2**, 397-400, 1997.

Smart, D.F, M.A. Shea, and E.O. Flückiger, Calculated vertical cosmic ray cutoff rigidities for the International Space Station during magnetically quiet times, *Proc. 26th ICRC*, **7**, 394-397, 1999a.

Smart, D.F. M.A. Shea, E.O. Flückiger, A. Tylka, and P.R. Boberg, Calculated vertical cosmic ray cutoff rigidities for the International Space Station during magnetically active times, *Proc. 26th ICRC*, **7**, 398-401, 1999b.

Smart, D.F. M.A. Shea, E.O. Flückiger, A. Tylka, and P.R. Boberg, Changes in calculated vertical cutoff rigidities at the altitude of the International Space Station as a function of magnetic activity, *Proc. 26th ICRC*, **7**, 337-340, 1999c.

Tsyganenko, N.A., Determination of magnetospheric current system parameters and development of experimental geomagnetic filed models based on data from IMP and HEOS satellites, *Planet. Space Sci.*, **37**, 5-20, 1989.